

Effects of an electric field on Feshbach resonances and the thermal-average scattering rate of ${}^6\text{Li}$ - ${}^{40}\text{K}$ collisions

Ting Xie, Gao-Ren Wang, Wei Zhang, Yin Huang, and Shu-Lin Cong*

School of Physics and Optoelectronic Technology, Dalian University of Technology, Dalian 116024, China

(Received 26 July 2012; published 26 September 2012)

The effects of an electric field on the magnetically induced ${}^6\text{Li}$ - ${}^{40}\text{K}$ Feshbach resonances are investigated theoretically by using the asymptotic bound-state model. We calculate the positions and widths of the Feshbach resonances observed in the experiments in the presence of an electric field and give a detailed analysis. An electric field can change the relative magnetic moment and the coupling strength to a different extent. The variation of resonant width caused by a strong electric field mainly depends on the coupling strength, and the s -wave scattering cross section in an electric field is sensitive to the temperature of the colliding system and the magnetic-field intensity. The maximum of the thermal average scattering rate constant can be changed by several factors by applying an electric field.

DOI: [10.1103/PhysRevA.86.032713](https://doi.org/10.1103/PhysRevA.86.032713)

PACS number(s): 34.50.Cx, 67.85.-d

I. INTRODUCTION

The Feshbach resonance is a useful tool for controlling the atom-atom interaction in ultracold atom gases [1–4]. By changing the magnetic field around resonance, the s -wave scattering length, which is a measure of the strength of the interaction, can be obtained using arbitrary values [5,6]. Meanwhile, the elastic scattering cross section can be enhanced by several orders. Recent theoretical works have demonstrated that a static electric field can induce Feshbach resonance in heteronuclear mixtures of atomic gases [7–11]. The mechanism stems from the interaction of the instantaneous dipole moment of a heteronuclear collision complex with the external electric field. This anisotropic interaction couples the states of different orbital angular momenta. The coupling between the open-channel and closed-channel bound states can change the width of Feshbach resonance to some degree.

Wille *et al.* observed the Feshbach resonances in an ultracold mixture of ${}^6\text{Li}$ and ${}^{40}\text{K}$ and found some resonances below 300 G [12]. The combination of ${}^6\text{Li}$ and ${}^{40}\text{K}$ fermionic alkali-metal species is a prime candidate for realizing strongly interacting Fermi-Fermi systems. Tiecke *et al.* calculated the widths and positions of all available Feshbach resonances for a ${}^6\text{Li}$ and ${}^{40}\text{K}$ collision complex using the asymptotic bound-state model (ABM) [13,14]. Naik *et al.* particularly researched the inelastic scattering properties and provided the essential information to identify optimum resonances for applications relying on interaction control in this Fermi-Fermi mixture [15]. They also proposed a way to create ultracold ${}^6\text{Li}$ - ${}^{40}\text{K}$ molecules. Since the LiK molecule has a relatively large permanent dipole moment in its ground electronic state, it is a good candidate for researching the effect of a static electric field on the Feshbach resonance.

Recently we investigated the external electric-field modulation of the magnetically induced ${}^6\text{Li}$ - ${}^{40}\text{K}$ Feshbach resonances using the extended ABM [11]. In this paper, we investigate the effects of an external electric field on magnetically induced ${}^6\text{Li}$ - ${}^{40}\text{K}$ Feshbach resonances, including the resonant position and width, the scattering cross section, and the thermal average

rate constant, and give a detailed analysis about the interaction mechanism in order to interpret experimental results. In Sec. II, we briefly introduce the ABM theory including an external electric field. In Sec. III, we discuss the influences of an electric field on all observable Feshbach resonances for the ${}^6\text{Li}$ - ${}^{40}\text{K}$ collision complex in experiments. In Sec. IV, a conclusion is drawn.

II. THEORETICAL APPROACH

The ABM has been successfully used to predict the magnetic-field position and width of the Feshbach resonance [11]. In the following, we demonstrate how the ABM can be used to determine the energy of the coupled molecular states and the eigenstates of the total Hamiltonian \hat{H} , without solving the actual coupled radial Schrödinger equation. For the collision of two atoms in external magnetic and electric fields the total Hamiltonian is given by

$$\hat{H} = \frac{\mathbf{p}^2}{2\mu} + \hat{H}_{\text{int}} + \hat{V}(R) + \frac{\hat{l}^2}{2\mu R^2} + \hat{V}_\zeta(R), \quad (1)$$

where $\frac{\mathbf{p}^2}{2\mu}$ represents the relative kinetic energy with μ being the reduced mass and \hat{H}_{int} is the two-body internal energy determined by the hyperfine and Zeeman interactions. The direction of magnetic field \mathbf{B} is chosen to be along the quantization z axis. H_{int} can be expressed as [14]

$$\begin{aligned} \hat{H}_{\text{int}} &= \hat{H}_{\text{int}}^\alpha + \hat{H}_{\text{int}}^\beta \\ &= \frac{a_{\text{hf}}^\alpha}{\hbar^2} I_\alpha S_\alpha + (\gamma_e M_{S_\alpha} - \gamma_I^\alpha M_{I_\alpha}) B + \frac{a_{\text{hf}}^\beta}{\hbar^2} I_\beta S_\beta \\ &\quad + (\gamma_e M_{S_\beta} - \gamma_I^\beta M_{I_\beta}) B, \end{aligned} \quad (2)$$

where S_α (S_β) and I_α (I_β) are the electronic and nuclear spins for atom α (β), respectively, and γ_e and γ_I^α (γ_I^β) are the respective gyromagnetic ratios. a_{hf}^α (a_{hf}^β) denotes the hyperfine energy for atom α (β). M_{S_α} (M_{S_β}) and M_{I_α} (M_{I_β}) are the electronic and nuclear magnetic quantum numbers of atom α (β), respectively. The hyperfine interaction describes the coupling between the electronic and nuclear spins, resulting in

*shlcong@dlut.edu.cn

a total angular momentum $f_\alpha = S_\alpha + I_\alpha$ ($f_\beta = S_\beta + I_\beta$) for atom α (β).

The Coulomb interaction potential $\hat{V}(R)$ depends on the total electronic spin $S = S_\alpha + S_\beta$ and interatomic distance R . It can be expressed as [8]

$$\hat{V}(R) = \sum_{SM_S} |SM_S\rangle V_S(R) \langle SM_S|, \quad (3)$$

where $V_S(R)$ is the adiabatic molecular potential of the collision complex in the spin state S . The centrifugal potential $\frac{\hbar^2 l^2}{2\mu R^2}$ and Coulomb potential form the effective potentials $V_S^l(R)$, where l denotes the rotational quantum number.

The operator $\hat{V}_\zeta(R)$, describing the electric-field-complex interaction, can be written as [7]

$$\hat{V}_\zeta(R) = -\vec{\zeta} \cdot \vec{d} = -\zeta(\hat{e}_\zeta \cdot \hat{e}_d) \sum_{SM_S} |SM_S\rangle d_S(R) \langle SM_S|, \quad (4)$$

where \hat{e}_ζ and \hat{e}_d represent the unit vectors of the electric field and the dipole moment, respectively. ζ is the electric-field magnitude and $d_S(R)$ the spin-dependent dipole moment of the collision complex. The dipole moment is given by [10]

$$d_S(R) = D_S \exp[-\alpha_S(R - R_e^S)^2], \quad (5)$$

with the parameters $R_e^0 = 7.5a_B$, $\alpha_0 = 0.0406a_B^2$, and $D_0 = 3.807$ D for the singlet state, and $R_e^1 = 5.3a_B$, $\alpha_1 = 0.105a_B^2$, and $D_1 = 0.95$ D for the triplet state, where the Bohr radius is $a_B = 0.0529177$ nm. The numerical data of dipole moments calculated by Aymar and Dulieu [16] are fitted well to the above analytical expression.

In the ABM, the Schrödinger equation for Hamiltonian (1) is solved starting from a restricted set of discrete eigenstates $|\psi_\nu^{SI}\rangle$ of relative motion of two-body composed of the kinetic energy and Coulomb potential including the centrifugal potential, using binding energy ϵ_ν^{SI} as a free parameter. The set of $\{|\psi_\nu^{SI}\rangle\}$ corresponds to the bound-state wave functions in the effective potentials $V_S^l(r)$, with ν being vibrational quantum numbers.

We specify the ABM basis states as $\{|\psi_\nu^{SI}\rangle|\sigma m_l\rangle\}$, where the spin basis states $|\sigma\rangle = |SM_S M_{I_\alpha} M_{I_\beta}\rangle$ and m_l denotes the magnetic quantum number corresponding to the orbital angular momentum l . The sum $M_F = M_S + M_{I_\alpha} + M_{I_\beta}$ is a conserved quantity and limits the number of spin states in the basis set.

The matrix elements of $\hat{V}_\zeta(R)$ are evaluated by using the expression

$$\langle\psi|\langle l m_l|\hat{V}_\zeta|l' m'_l\rangle|\psi'\rangle = \zeta\langle\psi_\nu^{SI}|d_S(R)|\psi_\nu^{SI'}\rangle\langle l m_l|\hat{e}_\zeta \cdot \hat{e}_d|l' m'_l\rangle, \quad (6)$$

where $\langle\psi_\nu^{SI}|d_S(R)|\psi_\nu^{SI'}\rangle = \int_0^\infty (\psi_\nu^{SI})^* d_S(R) \psi_\nu^{SI'} dR$ is defined as the transition factor from $|l\rangle$ to $|l'\rangle$ in this paper. Since it depends on interatomic distance R , the eigenfunctions of bound state $\{|\psi_\nu^{SI}\rangle\}$ need to be precalculated by using the mapped Fourier grid method [17–19]. The coupling between an electric field and a dipole moment depends on the angle χ between them, that is, $\hat{e}_\zeta \cdot \hat{e}_d = \cos\chi$. It is convenient to define two angles γ and θ as follows: γ is the angle between the electric field and quantization z axis, and θ is the angle between dipole moment and the z axis. The angular calculation can be expressed as

$$\begin{aligned} \langle l m_l|\hat{e}_\zeta \cdot \hat{e}_d|l' m'_l\rangle &= \frac{1}{\sqrt{2}} \sin\gamma (-1)^{m'_l} \sqrt{(2l+1)(2l'+1)} \begin{pmatrix} l & 1 & l' \\ 0 & 0 & 0 \end{pmatrix} \begin{pmatrix} l & 1 & l' \\ m_l & -1 & -m'_l \end{pmatrix} \\ &+ \cos\gamma (-1)^{m'_l} \sqrt{(2l+1)(2l'+1)} \begin{pmatrix} l & 1 & l' \\ 0 & 0 & 0 \end{pmatrix} \begin{pmatrix} l & 1 & l' \\ m_l & 0 & -m'_l \end{pmatrix} \\ &- \frac{1}{\sqrt{2}} \sin\gamma (-1)^{m'_l} \sqrt{(2l+1)(2l'+1)} \begin{pmatrix} l & 1 & l' \\ 0 & 0 & 0 \end{pmatrix} \begin{pmatrix} l & 1 & l' \\ m_l & 1 & -m'_l \end{pmatrix}. \end{aligned} \quad (7)$$

To determine the characteristic properties of Feshbach resonances including the widths and positions, we need to examine the behavior of the coupled bound states near the threshold of an open channel. By comparing the total energy with channel threshold which is determined by the internal energy of the collision complex, we can distinguish the open from the closed channels. Then the Hilbert space can be partitioned into open- and closed-channel subspaces [20,21]. The Hamiltonian of the collision system is written as

$$\hat{H} = \hat{H}_{PP} + \hat{H}_{QQ} + \hat{H}_{PQ} + \hat{H}_{QP}, \quad (8)$$

with $\hat{H}_{PP} = \hat{P}\hat{H}\hat{P}$ and $\hat{H}_{QQ} = \hat{Q}\hat{H}\hat{Q}$ and $\hat{H}_{PQ} (= \hat{H}_{QP}^\dagger) = \hat{P}\hat{H}\hat{Q}$, where \hat{P} and \hat{Q} are projection operators of the open- and closed-channel subspaces, respectively. \hat{H}_{PQ} provides a measure for the coupling between the open P channel and the closed Q channel.

In order to calculate the width of a Feshbach resonance, three quantities are required: the binding energy ϵ_P of the open channel, the energy ϵ_Q of the closed channel responsive to the Feshbach resonance, and the coupling matrix element \mathcal{K} between the two channels. Since the width ΔB is defined as the difference in magnetic fields between $a = 0$ and $a = \infty$, we define a S matrix as $S = S_P S_Q$, where S_P denotes the direct scattering matrix describing the scattering process in the P space and S_Q is the resonance scattering matrix. In the case without shape resonance, if one open channel is coupled to a single closed channel in the vicinity of a resonance, the S_Q matrix can be expressed as [22,23]

$$S_Q = 1 - 2\pi i \frac{|\langle\phi_Q|H_{QP}|\Psi_P^+\rangle|^2}{E - \epsilon_Q - \gamma(E)}, \quad (9)$$

where ϕ_Q is the eigenstate of \hat{H}_{QQ} and Ψ_P^+ denotes the scattering eigensate of \hat{H}_{PP} . The collision energy $E =$

$\hbar^2 k^2 / (2\mu)$ is defined with respect to the open-channel threshold energy. The complex energy shift $\gamma(E)$ describes the dressing of a bare bound state ϕ_Q by coupling to the P space.

Experimentally, the colliding complex is prepared in a hyperfine state. For an ultracold atomic collision, the energy thresholds of the open and closed channels can be determined by the Zeeman hyperfine interaction. Performing a basis transformation from the spin basis state $|\sigma\rangle$ to atomic hyperfine states $|f, m_f\rangle_\alpha \otimes |f, m_f\rangle_\beta$, we can distinguish the open- and closed-channel subspaces. In the case of one open channel, \hat{H}_{PP} is a single matrix element on the diagonal of \hat{H} , corresponding to the bare binding energy of the least bound state of the entrance channel, $\epsilon_P = -\hbar^2 \kappa_P^2 / (2\mu)$. Then we consider the second basis transformation in which the closed-channel subspace is diagonalized and the open-channel subspace keeps unchanged. We obtain the eigenstates of \hat{H}_{QQ} and are able to identify the bound state responsive to a particular Feshbach resonance. The one-dimensional P space is not changed by the basis transformation. Using the basis of eigenstates of \hat{H}_{PP} and \hat{H}_{QQ} , we easily find the coupling matrix element $\mathcal{K} = \langle \phi_P | \hat{H}_{PQ} | \phi_{Q_i} \rangle$, where $|\phi_P\rangle$ denotes the bare bound state in the P space and $|\phi_{Q_i}\rangle$ is the i th bound state with binding energy ϵ_{Q_i} ($i = 1, 2, \dots$) in the Q space. The resonant width ΔB can be expressed as [14]

$$\Delta B = \frac{1}{a_{\text{bg}}} \frac{\mathcal{K}^2}{2\kappa_P |\epsilon_P| \mu_{\text{rel}}}. \quad (10)$$

The background scattering length $a_{\text{bg}} = a_{\text{bg}}^P + a^P$, where $a_{\text{bg}}^P \approx \frac{1}{2} \left(\frac{2\mu C_6}{\hbar} \right)^{1/4}$ and $a^P = \kappa_P^{-1}$. μ_{rel} is the relative magnetic moment of the collision complex between the open and the closed channels. The resonant position is related to the crossing of uncoupled bound state (B'_0) with the threshold [14]

$$B_0 = B'_0 + \frac{\mathcal{K}^2}{2\mu_{\text{rel}} |\epsilon_P|}. \quad (11)$$

The scattering length can be expressed as

$$a(B) = a_{\text{bg}} \left(1 - \frac{\Delta B}{B - B_0} \right). \quad (12)$$

Until now we have considered only the scattering at $T = 0$. However, even at ultralow temperature the finite temperature plays a significant role. In the following description, the influence of temperature on scattering amplitude and cross section is taken into account. The s -wave scattering amplitude f_0 is expressed as

$$f_0 = \frac{1}{k} e^{i\eta_0} \sin \eta_0 = \frac{1}{k \cot \eta_0 - ik}, \quad (13)$$

where η_0 is the s -wave phase shift and $k = \sqrt{2\mu k_B T / \hbar^2}$, with k_B being the Boltzmann constant and T being the temperature of the collision complex. The s -wave scattering cross section $\sigma(k)$ is given by

$$\sigma(k) = 4\pi |f_0|^2 = 4\pi \frac{1}{k^2 \cot^2 \eta_0 + k^2}. \quad (14)$$

In the absence of shape resonance we can express an energy-dependent s -wave phase shift as

$$\eta_0(E) = -ka_{\text{bg}} - \arg(-\delta + ik\Omega) = \eta_{\text{bg}}(E) + \eta_{\text{res}}(E), \quad (15)$$

where $\Omega = \frac{\mathcal{K}^2}{2\kappa_P |\epsilon_P|}$ corresponds to the coupling strength between the open and the closed channels and $\delta = \mu_{\text{rel}}(B - B_0) - E$ is the detuning from the resonance. The resonant phase shift is given by

$$\eta_{\text{res}}(E) = \arctan \left(-k \frac{a_{\text{bg}} \Delta B \mu_{\text{rel}}}{E - \mu_{\text{rel}}(B - B_0)} \right). \quad (16)$$

Assuming the nonresonant phase shift $\eta_{\text{bg}}(E) = -ka_{\text{bg}} \simeq -\tan ka_{\text{bg}}$ in the case of ultralow temperature, we can obtain the energy-dependent scattering cross section

$$\sigma(k) = \frac{4\pi}{k^2} \frac{(k\Omega - ka_{\text{bg}}\delta)^2}{(1 + k^2 a_{\text{bg}}^2)(\delta^2 + k^2 \Omega^2)}. \quad (17)$$

To obtain a thermally averaged cross section we need to average all possible collision energy E . The collision rate $n\langle\sigma v\rangle$ is an important parameter in experiments, where n and $v = \sqrt{2E/\mu}$ are the density and the relative velocity of the collision complex, respectively. Since $\langle\sigma\rangle$ is independent of \mathbf{r} , we can obtain [24]

$$\langle\sigma v\rangle = \sqrt{\frac{8}{\pi \mu (k_B T)^3}} \int_0^\infty \sigma(E) E e^{-E/k_B T} dE. \quad (18)$$

The above expression can be given analytically when the Wigner law is valid [25].

III. RESULTS AND DISCUSSIONS

In the present work, we investigate the magnetically induced ${}^6\text{Li}$ - ${}^{40}\text{K}$ Feshbach resonances modulated by an external electric field. We neglect the weak dipole-dipole interaction and consider only s - and p -wave bound-state scatterings since the resonance induced by high-order coupling is very weak compared to the one induced by direct coupling [10,26]. The adiabatic molecular interaction potential $V_S(R)$ is adopted from Ref. [27]. The transition factors we calculated are 406.181 and 23.219 cm^{-1} for the singlet and triplet states, respectively.

First, we distinguish two different s -wave resonances: the intrinsic s -wave resonance which exists in the absence of an electric field, and the electric-field-induced s -wave resonance which exists only in the presence of an electric field. In order to investigate the mechanism of electric-field modulation of the magnetically induced Feshbach resonance, we calculate the positions and widths of the Feshbach resonances observed in experiments at $\zeta = 100$ kV/cm in Table I, where the electric field is directed along the z axis. The inelastic losses caused by coupling to the p -wave open channel can be neglected since we choose the energetically lowest spin combination. In the case of an initial s wave, there is one s -wave channel that is energetically open. The s -wave resonances shift to different directions and the shifts are irregular. Specially, two of electric-field-induced s -wave resonances at 13.9 G for $M_F = -3$ and 17.5 G for $M_F = -2$ shift quickly to a lower magnetic field.

TABLE I. Survey of s -wave resonances of ${}^6\text{Li}$ - ${}^{40}\text{K}$ in an external electric field. The first four columns list the total angular momentum projections M_F , the hyperfine states of ${}^6\text{Li}$ and ${}^{40}\text{K}$, the resonant positions B_0 and widths ΔB in the absence of an electric field in experiments. For all resonances, $f_{\text{Li}} = 1/2$ and $f_{\text{K}} = 9/2$. Here we present the atomic hyperfine states in which the resonances have been observed in experiments [12,13]. Note that the experimental width of the loss feature ΔB_{expt} is not the same as the field width ΔB of the scattering length singularity. The resonant positions we calculated agree well with the experimental results. The last two columns give the variations of resonant positions and the widths at $\zeta = 100$ kV/cm. Since the p -wave resonance can induce the s -wave resonance in the presence of an electric field, we also give the variations of electric-field-induced resonances in the last two columns.

M_F	$m_{f_{\text{Li}}}, m_{f_{\text{K}}}$	Experiment		Theory			
		B_0 (G)	ΔB_{expt} (G)	B_0 (G)	ΔB (G)	Shift (G)	$\Delta B' - \Delta B$ (G)
-5	-1/2, -9/2	215.5	1.7	215.6	0.16	12.75	0.012
-4	+1/2, -9/2	157.6	1.7	157.6	0.08	-6.02	-0.015
-4	+1/2, -9/2	168.2	1.2	168.5	0.08	8.17	-0.002
-4	+1/2, -9/2	249.0	11.0	244.3	p wave	6.53	0.025
-3	+1/2, -7/2	16.1	3.8	13.9	p wave	-13.33	<0.0001
-3	+1/2, -7/2	149.2	1.2	149.1	0.12	-5.87	-0.041
-3	+1/2, -7/2	159.5	1.7	159.7	0.31	6.42	0.025
-3	+1/2, -7/2	165.9	0.6	165.9	0.0005	5.98	0.0007
-3	+1/2, -7/2	263.0	11.0	260.7	p wave	6.47	0.024
-2	+1/2, -5/2	Not observed		17.5	p wave	-16.77	<0.0001
-2	+1/2, -5/2	141.7	1.4	141.4	0.12	-5.07	-0.040
-2	+1/2, -5/2	154.9	2.0	154.8	0.50	4.89	0.024
-2	+1/2, -5/2	162.7	1.7	162.6	0.07	6.18	-0.012
-2	+1/2, -5/2	271.0	14.0	274.0	p wave	5.86	0.020
+5	+1/2, +9/2	114.47(5)	1.5(5)	115.9	0.91	-2.50	-0.240

Due to energy repulsion, the shift of s -wave resonance depends on the relative magnetic moment μ_{rel} . The resonances shift to high magnetic field when $\mu_{\text{rel}} > 0$, and shift to low magnetic field if $\mu_{\text{rel}} < 0$. Though the s -wave resonances in Table I possess the positive relative magnetic moments, they are situated at lower magnetic field and the energy level spacing between the s - and p -wave bound states are small compared to those at higher magnetic field. The widths of intrinsic s -wave resonances are changed slightly by the external electric field except for the resonances at 149.1 G for $M_F = -3$, 141.4 G for $M_F = -2$ and 115.9 G for $M_F = 5$. Moreover, we can see that three electric-field-induced Feshbach resonances at 244.3 G for $M_F = -4$, 260.7 G for $M_F = -3$, and 274 G for $M_F = -2$ are greater than or equal to 0.02 G at $\zeta = 100$ kV/cm, which may be easily observed in experiment. However, the widths of two s -wave resonances induced by an electric field at 13.9 G for $M_F = -3$ and 17.5 G for $M_F = -2$ are very small, <0.0001 G and are hardly observed.

According to Eq. (10), the width of a Feshbach resonance in the presence of an electric field is determined directly by the relative magnetic moment μ_{rel} and the coupling strength \mathcal{K} because the open-channel energy is hardly changed by the electric field [11]. To further research the effect of an electric field on the width, we plot μ_{rel} , \mathcal{K}^2 , and resonant width in the atomic spin state $|\frac{1}{2}, \frac{1}{2}\rangle_{\text{Li}} \otimes |\frac{9}{2}, -\frac{5}{2}\rangle_{\text{K}}$ as a function of electric-field intensity in Fig. 1. In the presence of an electric field with $\gamma = 0$, there are five s -wave resonances. Two of them, at A_S and E_S , are the Feshbach resonances induced by an electric field and the others are intrinsic resonances. In Fig. 1(a), the relative magnetic moments for the resonances at

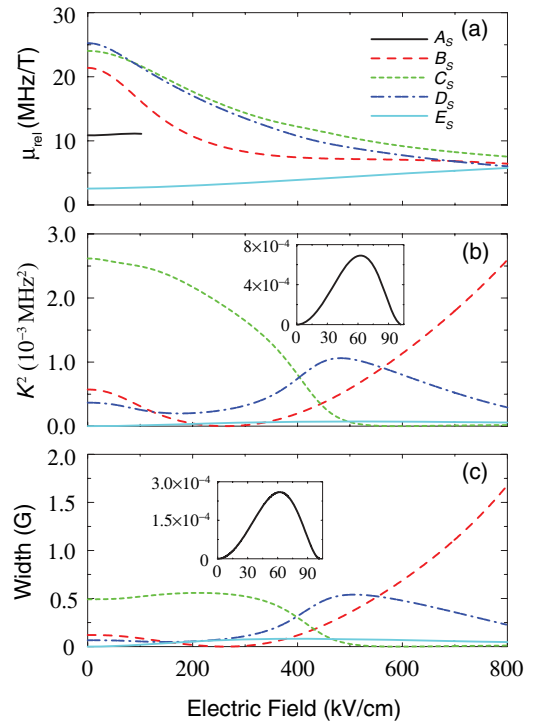


FIG. 1. (Color online) The relative magnetic moment μ_{rel} , the square of coupling strength \mathcal{K} , and the resonant width versus the electric-field intensity. In the presence of an electric field, five s -wave resonant positions $A_S \sim E_S$ in the atomic spin state $|\frac{1}{2}, \frac{1}{2}\rangle_{\text{Li}} \otimes |\frac{9}{2}, -\frac{5}{2}\rangle_{\text{K}}$ are labeled in the order of increasing magnetic field. Note that the resonance at A_S shift to lower magnetic field with increasing electric-field intensity and vanishes when $\zeta \geq 105$ kV/cm.

B_S , C_S , and D_S decrease with increasing electric-field intensity and vary slowly when $\zeta > 500$ kV/cm. This is because the relative magnetic moment is directly related to the energy of the bound state, $\mu_{\text{rel}} = \partial \epsilon_Q / \partial B|_{B=B_0}$. The energies of s -wave and p -wave bound states related to these resonances are very close to each other. A weak electric field can modify the energies of s -wave and p -wave bound states and result in an avoided crossing between them. By increasing the electric-field intensity, the resonances shift away from the avoided crossing and the energy spacing between the s - and the p -wave bound states increases at the resonant positions. The effect of electric field on the energies of the bound states and the relative magnetic moment μ_{rel} are changed slowly. While the relative magnetic moments at A_S and E_S increase slowly with increasing electric-field intensity since the energy spacing between the s - and p -wave bound states related to the two resonances are large enough in the absence of an electric field.

The electric field cannot only change the relative magnetic moment of the collision complex; it can also change the coupling strength between the open channel bound state and the closed-channel bound state which is responsive to the Feshbach resonance. Figure 1(b) shows the square of coupling strength versus the electric-field intensity. The curves do not exhibit a monotonic variation since the energies of both dressed and uncoupled bound states are modified by the electric field by varying degrees. The coupling strengths associated to the resonances at A_S and E_S reach their respective maxima and then decrease with the increase of electric-field intensity. We also observe the variation of coupling strength for all five electric-field-induced s -wave resonances listed in Table I and find they exhibit similar behavior. This can be explained as follows: A strong electric field can enhance the coupling between the s -wave and p -wave bound states. However, it can also shift the position of Feshbach resonance at which the Zeeman interaction is changed. When the electric field is weak, the shift of Feshbach resonance is small and the coupling between the s -wave and p -wave bound states mainly depends on electric-field intensity. In a strong electric field, $\zeta > 200$ kV/cm, the shift of Feshbach resonance nearly linearly changes with the electric-field intensity [11] and the coupling strength depends on the Zeeman interaction and the electric-field-complex interaction. The two interactions have opposite effects on the coupling strength related to the electric-field-induced resonances for ${}^6\text{Li}$ - ${}^{40}\text{K}$, which leads to the decrease of the coupling strength with increasing the electric-field intensity.

Since the energy of open channel cannot be changed by an electric field, the variation trend of Feshbach resonant width is similar to that of $\mathcal{K}^2/\mu_{\text{rel}}$. Figure 1(c) shows the resonant width versus electric-field intensity. By observing Fig. 1, we conclude that the electric field can change μ_{rel} and \mathcal{K}^2 to a different extent, and the strong electric field can more obviously influence \mathcal{K}^2 than μ_{rel} .

Figure 2 displays the changes of s -wave scattering cross section with electric-field intensity in different magnetic fields in the atomic spin state $|\frac{1}{2}, \frac{1}{2}\rangle_{\text{Li}} \otimes |\frac{9}{2}, -\frac{5}{2}\rangle_{\text{K}}$. The resonance feature in Figs. 2(a) and 2(b) is the shift of intrinsic magnetic Feshbach resonance at C_S shown in Fig. 1 to a higher magnetic field, and the resonance feature in Figs. 2(c) and 2(d) is the

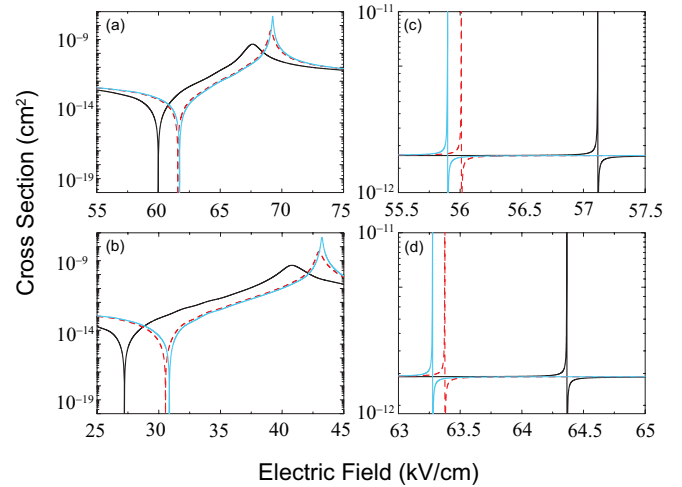


FIG. 2. (Color online) The electric-field dependence of s -wave scattering cross section in the atomic spin state $|\frac{1}{2}, \frac{1}{2}\rangle_{\text{Li}} \otimes |\frac{9}{2}, -\frac{5}{2}\rangle_{\text{K}}$ in different magnetic fields: (a) $B = 160$ G, (b) $B = 158$ G, (c) $B = 12$ G, and (d) $B = 10.5$ G. The temperature of the collision complex is $12 \mu\text{K}$ (black solid lines), $1.2 \mu\text{K}$ (red dashed lines), and 120 nK (light blue lines).

shift of an electric field-induced resonance at A_S shown in Fig. 1 to a lower magnetic field when the electric-field intensity increases. For the case of representation, we define the resonant position ζ_0 and width $\Delta\zeta$ for the s -wave scattering in an electric field as $a = \infty$ and the difference between $a = 0$ and $a = \infty$, respectively. From Fig. 2, we can see that the resonant positions ζ_0 are shifted for $k > 0$ and converge at the temperature of nK. We also find the temperature of the collision complex (or collision energy) has different influences on the resonant positions at different magnetic-field intensities and the shifts of ζ_0 depend on μ_{rel} of the collision complex. At $T = 12 \mu\text{K}$, the shifts of resonant positions in the electric field are 2.4, 1.6, 1.2, and 1.0 kV/cm at $B = 158, 160, 12,$ and 10.5 G in order. The relative magnetic moments corresponding to magnetically induced resonances at $B = 158, 160, 12,$ and 10.5 G decrease in turn. So temperature has a significant influence on ζ_0 for a larger μ_{rel} . The resonant position and width in an electric field can be changed to a great extent by changing magnetic-field intensity. At the temperature of nK, the resonant positions are situated at $\zeta_0 = 69.25$ and 43.22 kV/cm for $B = 160$ and 158 G, respectively. The resonant position shift in an electric field caused by a magnetic field is 26 kV/cm and the resonant width is also changed obviously. However, not all s -wave resonances are sensitive to the magnetic-field intensity. At the temperature of nK, the resonant positions are located at 55.90 and 63.27 kV/cm for $B = 12$ and 10.5 G, respectively, and the widths are nearly the same. The resonant positions and widths in an electric field at different magnetic-field intensities are related to ΔB and B_0 , as shown in Fig. 1(c). When a magnetic Feshbach resonance is shifted by an electric field at a speed of $\frac{dB_0}{d\zeta}$, the corresponding resonance in an electric field is shifted by a magnetic field at a speed of $\frac{d\zeta_0}{dB} (= \frac{d\zeta}{dB_0})$. The resonance at A_S is shifted by an electric field more quickly than the resonance at C_S . As a result, the resonant positions in Fig. 2(a) can be obviously changed by slightly varying the magnetic field. In the case of ΔB unchanged, $\Delta\zeta$

is mainly determined by $\frac{d\zeta}{dB_0}$. From Fig. 1(c), the resonant width at A_S increases a little when ζ changes from 55.90 to 63.27 kV/cm. Similarly, the resonant width at C_S increases when ζ changes from 43.22 to 69.25 kV/cm. However, $\frac{d\zeta}{dB_0}$ is nearly unchanged at $B_0 = 10.5$ and 12 G, and increases 50% at $B_0 = 158$ G compared to the result at $B_0 = 160$ G. This provides an alternative way to steer the interatomic interaction by utilizing an external electric field.

Though an electric field can modify the scattering length, another interesting aspect in experiment is its effect on the scattering cross section, especially the thermal average cross section related to the collision rate. Figure 3 displays the scattering cross section at temperature $T = 12 \mu\text{K}$ and the thermal average rate constant in the atomic spin state $|\frac{1}{2}, \frac{1}{2}\rangle_{\text{Li}} \otimes |\frac{9}{2}, \frac{9}{2}\rangle_{\text{K}}$ as a function of magnetic-field intensity in different electric fields with $\gamma = 0$. With increasing the electric-field intensity, the resonant width becomes small and the maximum of scattering cross section is nearly unchanged. However, the maximum of the thermal average rate constant decreases with increasing electric-field intensity. In our calculation, the maximum of $\langle\sigma v\rangle$ at $\zeta = 200$ kV/cm approximately decreases to one-third of the value in the absence of an electric field. According to Eq. (17), at ultralow temperature the maximum of scattering cross section mainly depends on the wave vector k but not the resonant width, so it varies slightly under the action of an electric field. Since $\langle\sigma v\rangle$ is an average over all σv , its maximum is related to the resonant width. However, at a lower temperature, for example, nK, the effect of an electric field on the maximum of $\langle\sigma v\rangle$ weakens. This provides another interesting way to research the collision rate by applying an electric field.

The Fano profile of Feshbach resonance can be observed by measuring the distillation rate (or evaporation rate) of the Li from the K-rich Li-K mixture in the optical trap as

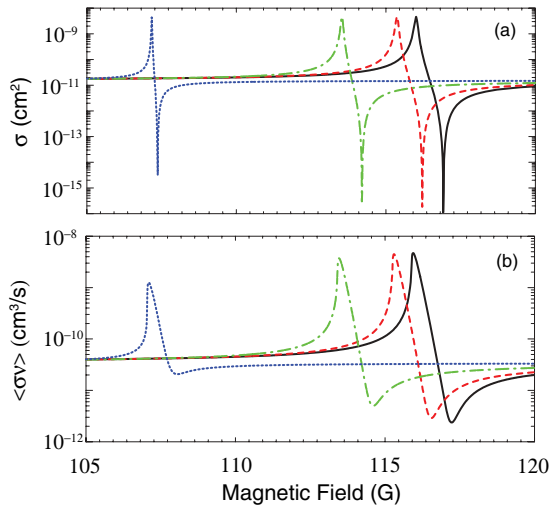


FIG. 3. (Color online) (a) The scattering cross section $\sigma(E)$ at temperature $T = 12 \mu\text{K}$ and (b) the corresponding thermal average scattering rate constant $\langle\sigma v\rangle$ in the atomic spin state $|\frac{1}{2}, \frac{1}{2}\rangle_{\text{Li}} \otimes |\frac{9}{2}, \frac{9}{2}\rangle_{\text{K}}$ as a function of magnetic-field intensity in different electric fields. The amplitudes of the electric fields are 0 kV/cm (black solid lines), 50 kV/cm (red dashed lines), 100 kV/cm (green dashed-dotted lines), and 200 kV/cm (blue dotted lines).

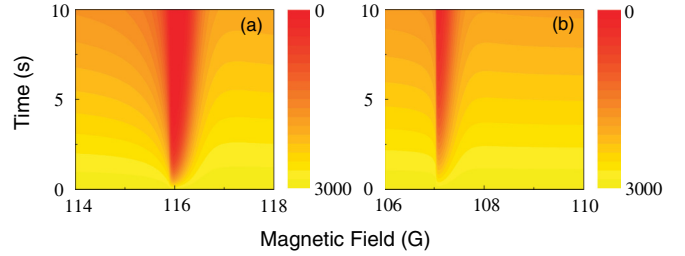


FIG. 4. (Color online) The number of Li atoms as a function of magnetic-field intensity and holding time t in the atomic spin state $|\frac{1}{2}, \frac{1}{2}\rangle_{\text{Li}} \otimes |\frac{9}{2}, \frac{9}{2}\rangle_{\text{K}}$ in electric fields (a) $\zeta = 0$ kV/cm and (b) $\zeta = 200$ kV/cm.

a function of magnetic-field intensity. We assume the Li evaporates at a rate proportional to the interspecies elastic cross section. Since the component of Li is minor in the Li-K mixture, this distillation process proceeds at an approximately constant rate. The distillation of Li as a function of time t is described by $N(t) = N_0 e^{-t/\tau_{\text{ev}}} e^{-t/\tau_{\text{bg}}}$, where $N_0 = 3 \times 10^3$ is the initial number of Li atoms, $\tau_{\text{bg}} = 25$ s the vacuum limited lifetime, and $\tau_{\text{ev}}^{-1} \simeq n_{\text{K}} \langle\sigma(k)\hbar k/\mu\rangle e^{-\eta_{\text{Li}}}$ the thermally averaged evaporation rate. $n_{\text{K}} = 2 \times 10^{11} \text{cm}^{-3}$ is the central density of the K atoms. $\eta_{\text{Li}} = 2.7$ is the truncation parameter of Li atoms after decompression. Figure 4 displays the distillation of Li atoms as a function of magnetic-field intensity and holding time in different electric fields. The resonant position and width can be determined by observing magnetic-field dependence of the number of Li atoms at different times. We can see the resonant position and width are obviously changed by an electric field. The losses of 50% and 15% in 1 s holding time at resonant positions for $\zeta = 0$ and 200 kV/cm are observed, respectively. Since the maximum of thermal average evaporation rate at $\zeta = 200$ kV/cm reduce to 1/3 of the value in the absence of an electric field, the distillation of Li atoms decreases. Moreover, the distillation of Li atoms also depends on the density of K atoms and the truncation parameter of Li atoms.

In the above discussion, the electric field is parallel to the magnetic field (angle $\gamma = 0$). Li *et al.* investigated the effect of nonparallel electric and magnetic fields on the Feshbach resonances [10]. They found the resonant position of the p -wave remains unchanged and the scattering cross section of the p -wave is nearly unchanged for different angle γ . We also study the effect of nonparallel electric and magnetic fields on the s -wave resonances ($\gamma \neq 0$). We find that the resonant position and width of the s -wave scattering are not influenced by γ . This is because the coupling between the s -wave and the p -wave bound states, which influences the s -wave resonant position and width, keeps unchanged for different γ . However, it is noteworthy that the nonparallel electric and magnetic fields may influence the transition from the open channel for the s wave to the open channels for the p wave. This needs to be further explored.

IV. CONCLUSION

We have investigated theoretically the effect of an electric field on the magnetic-field-induced Feshbach resonances for the ultracold ${}^6\text{Li}$ - ${}^{40}\text{K}$ collision complex using the ABM. The

relative magnetic moment can be changed by an electric field to varying degrees. The width of a Feshbach resonance in an electric field mainly depends on the coupling strength between the open-channel and the closed-channel bound states in a strong electric field. The s -wave scattering cross section in an electric field is sensitive to the temperature of the colliding complex and the magnetic-field intensity. The variation of temperature can cause a position shift of the maximal cross section in an electric field for a collision system with a larger magnetic moment. The resonant feature in an electric field can be changed to a great extent by slightly changing magnetic-field intensity. One can steer the interaction of heteronuclear molecules with a small permanent dipole moment

by utilizing an electric field and a magnetic field. An electric field can change the maximum of thermal average rate for the ultracold ${}^6\text{Li}$ - ${}^{40}\text{K}$ collision system by several times at the temperature of μK . However, at the temperature of nK , the effect of an electric field on the thermal average rate weakens.

ACKNOWLEDGMENTS

One of authors (T. Xie) gratefully acknowledges Z. Li for helpful discussions. This work is supported by the National Natural Science Foundation of China under Grant No. 10974024 and Specialized Research Fund for the Doctoral Program of Higher Education under Grant No. 20090041110025.

-
- [1] T. Weber, J. Herbig, M. Mark, H-C. Nägerl, and R. Grimm, *Science* **299**, 232 (2003).
- [2] I. Bloch, *Nature (London)* **453**, 1016 (2008).
- [3] C. Chin, R. Grimm, P. Julienne, and E. Tiesinga, *Rev. Mod. Phys.* **82**, 2 (2010).
- [4] Z. Li, *Phys. Rev. A* **81**, 012701 (2010).
- [5] T. Xie, G.-R. Wang, Y. Huang, W. Zhang, and S.-L. Cong, *J. Phys. B* **45**, 145302 (2012).
- [6] G.-R. Wang, T. Xie, W. Zhang, Y. Huang, and S.-L. Cong, *Phys. Rev. A* **85**, 032706 (2012).
- [7] R. V. Krems, *Phys. Rev. Lett.* **96**, 123202 (2006).
- [8] Z. Li and R. V. Krems, *Phys. Rev. A* **75**, 032709 (2007).
- [9] B. Marcellis, B. Verhaar, and S. Kokkelmans, *Phys. Rev. Lett.* **100**, 153201 (2008).
- [10] Z. Li and K. W. Madison, *Phys. Rev. A* **79**, 042711 (2009).
- [11] T. Xie, G.-R. Wang, W. Zhang, Y. Huang, and S.-L. Cong, *Phys. Rev. A* **84**, 032712 (2011).
- [12] E. Wille *et al.*, *Phys. Rev. Lett.* **100**, 053201 (2008).
- [13] T. G. Tiecke, M. R. Goosen, A. Ludewig, S. D. Gensemer, S. Kraft, S. J. J. M. F. Kokkelmans, and J. T. M. Walraven, *Phys. Rev. Lett.* **104**, 053202 (2010).
- [14] T. G. Tiecke, M. R. Goosen, J. T. M. Walraven, and S. J. J. M. F. Kokkelmans, *Phys. Rev. A* **82**, 042712 (2010).
- [15] D. Naik, A. Trenkwalder, C. Kohstall, F. M. Spiegelhalter, M. Zaccanti, G. Hendl, F. Schreck, R. Grimm, T. M. Hanna, and P. S. Julienne, *Eur. Phys. J. D* **65**, 55 (2011).
- [16] M. Aymar and O. Dulieu, *J. Chem. Phys.* **122**, 204302 (2005).
- [17] W. Zhang, Y. Huang, T. Xie, G.-R. Wang, and S.-L. Cong, *Phys. Rev. A* **82**, 063411 (2010).
- [18] W. Zhang, Z.-Y. Zhao, T. Xie, G.-R. Wang, Y. Huang, and S.-L. Cong, *Phys. Rev. A* **84**, 053418 (2011).
- [19] W. Zhang, T. Xie, Y. Huang, and S.-L. Cong, *Phys. Rev. A* **84**, 065406 (2011).
- [20] H. Feshbach, *Ann. Phys.* **5**, 357 (1958).
- [21] H. Feshbach, *Ann. Phys.* **19**, 287 (1962).
- [22] A. J. Moerdijk, B. J. Verhaar, and A. Axelsson, *Phys. Rev. A* **51**, 4852 (1995).
- [23] B. Marcellis, E. G. M. van Kempen, B. J. Verhaar, and S. J. J. M. F. Kokkelmans, *Phys. Rev. A* **70**, 012701 (2004).
- [24] T. Tiecke, Ph.D. thesis, Van der Waals-Zeeman Institute of the University of Amsterdam, 2009.
- [25] R. V. Krems and A. Dalgarno, *Phys. Rev. A* **67**, 050704(R) (2003).
- [26] C. J. Hemming and R. V. Krems, *Phys. Rev. A* **77**, 022705 (2008).
- [27] E. Tiemann, H. Knöckel, P. Kowalczyk, W. Jastrzebski, A. Pashov, H. Salami, and A. J. Ross, *Phys. Rev. A* **79**, 042716 (2009).